JOURNAL OF CHEMOMETRICS
J. Chemometrics 2000; **14**: 463–481

New developments in acoustic chemometric prediction of particle size distribution—'the problem is the solution'

Maths Halstensen and Kim Esbensen*

Applied Chemometrics Research Group (ACRG), Telemark College/Tel-Tek, Institute of Process Technology, Porsgrunn, Norway

SUMMARY

We present a new prototype acoustic chemometric approach for prediction of powder particle size distributions, intended for in-line implementation. The standard basic solutions demand that calibration be carried out on representative, 'non-segregated' reference powder samples. However, as practical powder flow with no segregation is extremely difficult to achieve with the precision needed for calibration, there will always be a significant uncertainty in the reference values relative to what is actually measured. *The problem is flow segregation*. In order to solve this problem, we have designed a completely new acoustic chemometric approach, which by way of contrast forces the flowing powder mass to segregate as much as possible by various mechanical means. The new approach measures the acoustic signals from an integrated series of segregated, part-sample characteristics. The calibration *X*-data matrix now becomes a three-way matrix, which demands a three-way calibration solution to 'unscramble' the latent information in the maximally segregated powder sample. Thus *the problem is now the solution*. Our earlier forays into this matter, which were based on two-way calibrations, have all been limited by a severe 'particle size ratio' bracket outside which destructive self-damping has effectively negated practical, useful accuracy and precision. The new approach allows a much greater range of contrasting particle sizes. Our first-generation results achieved by using three-way PLS-R as well as the standard two-way calibrations show that it is more precise than all earlier attempts and can be used for many-component mixtures without extensive further modifications. We also look at the feasibility of quantifying for prediction of in-line particle size distributions in an industrial environment. Copyright © 2000 John Wiley & Sons, Ltd.

KEY WORDS: three-way calibration; unfolding; PLS calibration; segregation; flow sampling; particle size distribution; acoustic chemometrics; sensor technology

INTRODUCTION

The applications of acoustic chemometrics are manifold [1–3]; quantitative analysis, process monitoring and physical characterization of products are some of the issues of immediate interest. Acoustic signals from appropriate sensors or directly from equipment monitors can be subjected to pertinent signal analysis and further chemometric data analysis.

Industrial processes cause heat, sound, vibration, etc. Emission of noise is characteristic of many such processes, usually in the form of incoherent acoustic energy output—also called noise. The noise shows up in the form of vibration energy, which however can be measured and characterized, and this

* Correspondence to: K. Esbensen, Applied Chemometrics Research Group (ACRG), Telemark College/Tel-Tek, Institute of Process Technology, Porsgrunn, Norway.

Copyright © 2000 John Wiley & Sons, Ltd.

Received 6 December 1999
Accepted 5 April 2000

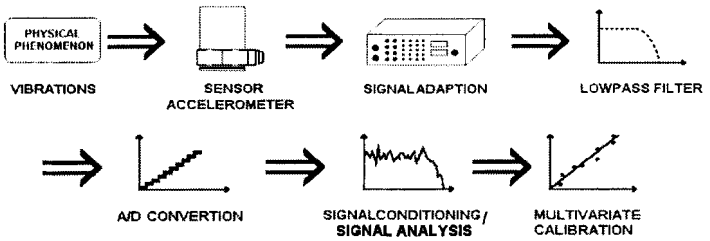

Figure 1. Generic data path flow sheet for acoustic chemometrics.

in turn can be subjected to our type of chemometric data analysis intended to reveal the hidden acoustic information. In this context, by acoustic output we mean vibration outputs in the frequency range 0–50 kHz. Acoustic particle size prediction can be made to fit into this overall scheme. By particle size we mean particles calibrated by a sieve with a particular square mesh size. By particle size distribution we mean a distribution showing the amount of particle sizes in each fraction—between two sieve mesh sizes—in a volume of particles.

In this paper we present some examples of new developments in applied acoustic chemometrics for monitoring particle size distributions. The irregular fluctuations that occur when powder reaches an acoustic sensor contain valuable information, which may be used to predict particle size distributions in powder mixtures.

Background

Acoustic chemometrics [1–3] can be applied in many different ways, but the common ground can be outlined in an overall simple-to-appreciate manner: the 'data path' from sound to information. Figure 1 is a schematic flow sheet for a generic acoustic chemometric data path, from the acoustic phenomenon to the final multivariate calibration model, including future prediction facilities.

The basic physical principle of acoustic particle size characterization concerns the kinetic impact of particles on the top surface of a suitable acoustic sensor. Particles with different kinetic impacts produce vibrations with different frequency characteristics. Figure 2 illustrates the correspondence between particle size and kinetic input energy; for mixtures containing particles of different sizes, the issue becomes more complex.

The acoustic sensor used in all present developments is a standard accelerometer covering the frequency range 0–20 kHz. The accelerometer used in these experiments is a standard 4396 accelerometer from Brüel & Kjær, shown in Figure 3 (right panel).

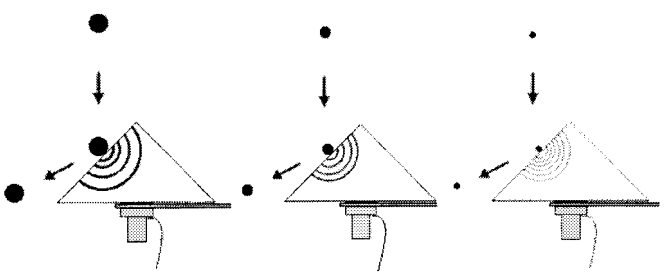

Figure 2. Particles (monophase) with different kinetic impacts produce vibrations with different frequency characteristics in the sensor head.

Copyright © 2000 John Wiley & Sons, Ltd.

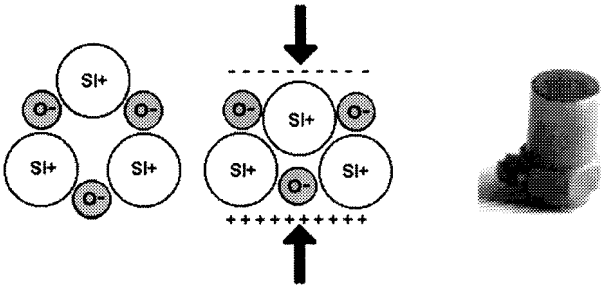

Figure 3. A quartz crystal (SiO_2) exposed to a compression force produces a negatively and a positively charged side. Right panel: Brüel & Kjær type 4396 accelerometer.

This type of sensor converts vibrations to an electric signal, which can be recorded with an appropriate digital acquisition interface. The fundamental working principle of the accelerometer is that of a dipole exposed to an alternating compression/tensional force. The atomic dipoles in the accelerometer's seismic mass (often quartz) will generate a positive and a negative charge on opposite surfaces of the measuring element, as illustrated in Figure 3. The material consists of many dipoles with the same orientation, and the charge will be large enough to be measured macroscopically and can conveniently be converted to a voltage signal.

The accelerometer measures continuous signals (as a function of time). In acoustic chemometrics, primary time series signals are converted from the time to the frequency domain by the FFT (fast Fourier transform) algorithm [4]. Figure 4 shows a typical FFT acoustic effect spectrum for the type of powder samples studied here. Our standard technology makes use of 0·04 s unit time recordings, a number of which may be aggregated to form statistically stable average measurements (e.g. 50, 100 replicates).

Such acoustic effect spectra from several reference particle size distributions can be used to calibrate a PLS-R (partial least squares regression) model [5]. When such a model is properly

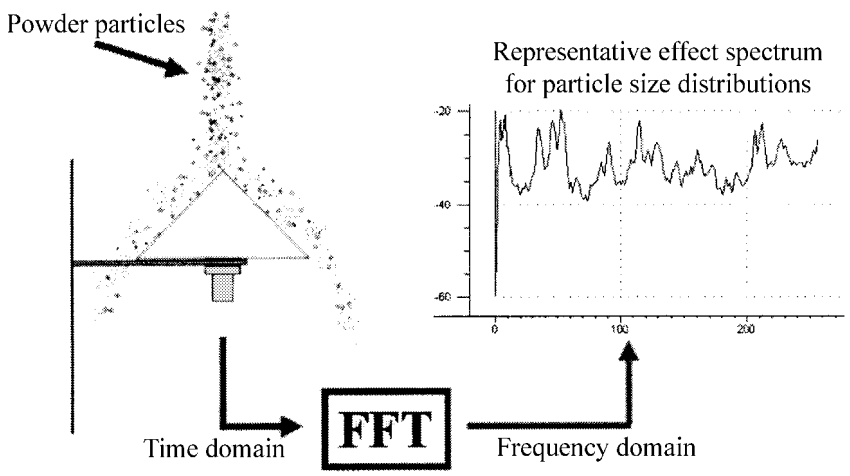

Figure 4. Time–frequency domain transformation by FFT (fast Fourier transform). Note the complexity of the flowing particle size distribution aggregate.

Copyright © 2000 John Wiley & Sons, Ltd.

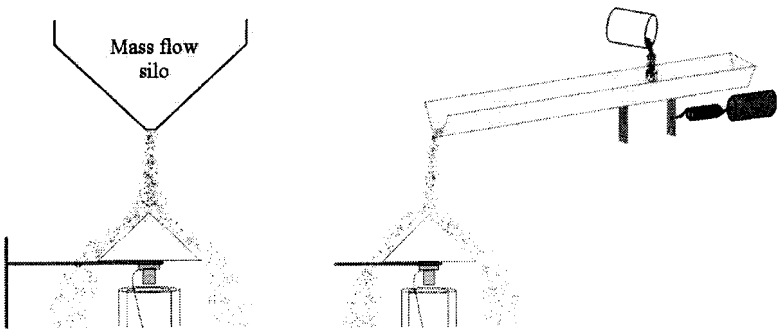

Figure 5. Experimental set-ups for the first generation of powder grain size experiments. Both set-ups are heavily influenced by flow segregation.

calibrated and validated, it can be used for prediction of particle size distributions from new acoustic effect spectra obtained with the same acoustic equipment.

HISTORICAL OVERVIEW

Experiments—basic approach

In the first generation of experiments, carried out some 5–8 years ago [6], two basic types of experimental sample delivery equipment were used, which have set the standard for all subsequent work.

1. Either a silo is used to establish a steady flow of particles onto the sensor head. This set-up can be seen in Figure 5 (left).
2. Alternatively, a vibrating slide is used to guide the particles to the acoustic sensor. This set-up can also be seen in Figure 5 (right).

Both cause significant flow segregation during the transport to the sensor.

The powder used in these earlier experiments was usually either a two-component or a three-component mixture consisting of non-overlapping size fractions A, B and C. A recent verification study of these experiments was carried out by Berdal [6], with a total number of experiments of 66. Figure 6 shows the complete experimental design [7] for a full three-component particle size mixture experiment with 10% increments.

For simple two-component systems the acoustic dominance of the larger particles will always carry the necessary information in order also to quantify the smaller particles. It is no problem to obtain very accurate and precise results for mixture series of two size fractions, provided there are no measurement problems present (especially provided there is no flow segregation present during sample delivery). However, the complexities of real-world, industrial applications demand at least three-component systems (four-, five-component systems). The three powder grain size fractions chosen for this experiment (Figure 6) consist of non-overlapping particle size fractions, with fractions A/B 'close' and fractions B/C only slightly more separated.

The acoustic data recorded for each of the 66 experiments were PLS modelled. The complete so-called 'predicted versus measured' validation plots, with accompanying statistics for all three fractions A, B and C, are shown in Figures 7–9. The models—shown in Figures 7–9—were validated by both full and segmented cross-validation procedures, with identical results.

A significant number of outliers had to be removed in these calibrations (seven, 22 and 13 respectively) because of measurement problems (flow segregation).

Copyright © 2000 John Wiley & Sons, Ltd.

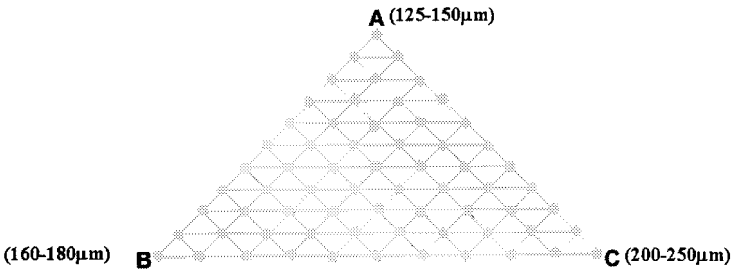

Figure 6. Experimental design for a three-component mixture series. Note non-overlapping size fractions A, B and C. Total no. of experiments: 66.

Figures 7–9 show that it is possible to predict particle size distributions with acoustic chemometrics—but also that the predicted values are certainly not very precise, only 5·7–10·2%. The highest precision is associated with the smallest grain size (5·7%).

Careful analysis of the entire calibration procedure identified one dominating source of imprecision: the quality of the *Y*-reference values. The problem concerns flow segregation [8] of the powder sample before it even reaches the acoustic sensor, so that the recorded signals are not representative with regard to the nominal reference values for the whole sample. Flow segregation is a well-known effect in powder transportation, which in many instances cannot be totally eliminated, but only suppressed in favourable situations. The dominating parameter which influences a flowing powder mixture to become segregated is the characteristic particle size ratio, *D/d* (*D*, diameter of large-particle-size fraction; *d*, diameter of small-particle-size fraction), as well as the vibration amplitude, flow speed, etc. The vibrating slide used in nearly all earlier work is segregation-prone (see Figure 10).

Each acoustic recording takes only 20 ms and the particle size distribution during this timeframe may not represent the total sample dumped into the end of the vibrating slide.

Thus the main problem with the earlier experiments was the uneven flow segregation of coarse and fine particles. The problem occurs when the particle size ratio is ‘too large’. At the microscale (see

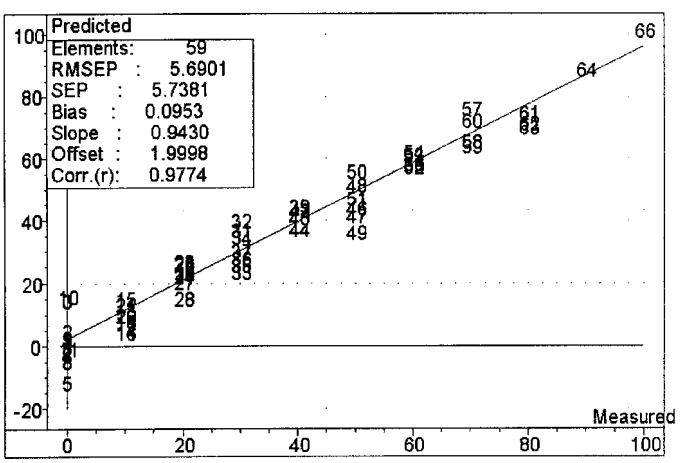

Figure 7. Predicted versus measured validation plot/statistics for fraction A.

Copyright © 2000 John Wiley & Sons, Ltd.

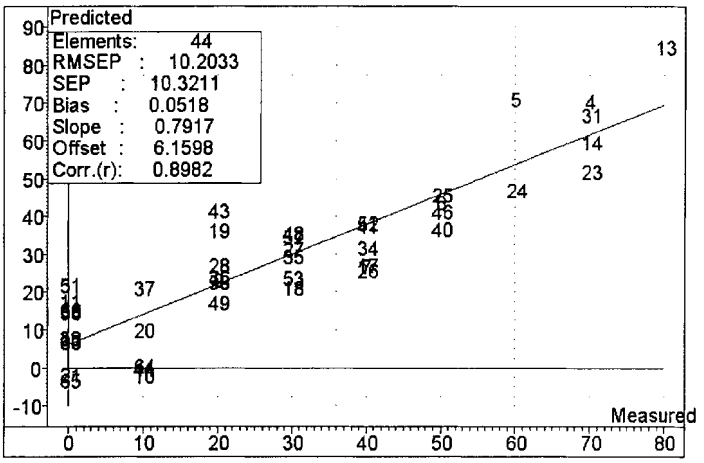

Figure 8. Predicted versus measured validation plot/statistics for fraction B.

Figure 2), acoustic signals from coarse particles will always dominate over those from the fine powder fractions, creating a distinct 'self-damping' effect w.r.t. the fine(r) fractions; this effect will always be present in what could be termed 'too large' *D/d* ratio situations. By 'too large' we mean $D/d > 2$ or so.

This problem can only be reduced by a variety of mechanical procedures, sensors, software, etc., but with little noticeable effect on the precision obtained. This *D/d* flow segregation problem relegated acoustic chemometric in-line particle size prediction to 'an interesting academic problem, impossible in practice' for many years.

Thus the problem was flow-induced, unavoidable segregation in the reference calibration as well as in the routine sample-measuring situations.

Enter a radical new approach (1999), however, according to the dictum: *the problem is the solution*.

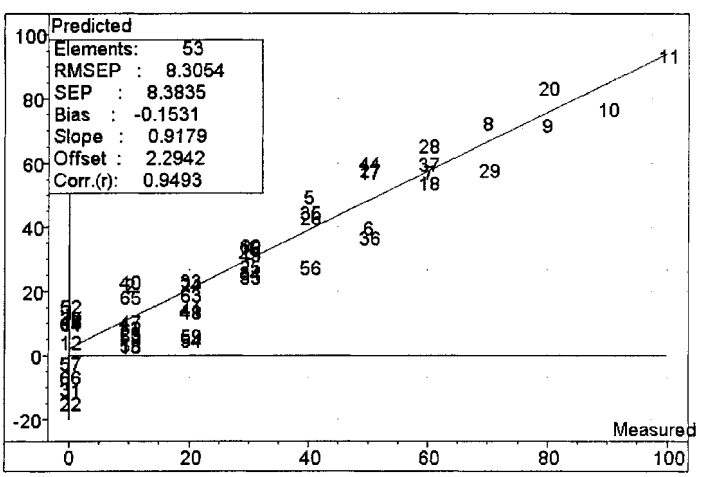

Figure 9. Predicted versus measured validation plot/statistics for fraction C.

Copyright © 2000 John Wiley & Sons, Ltd.

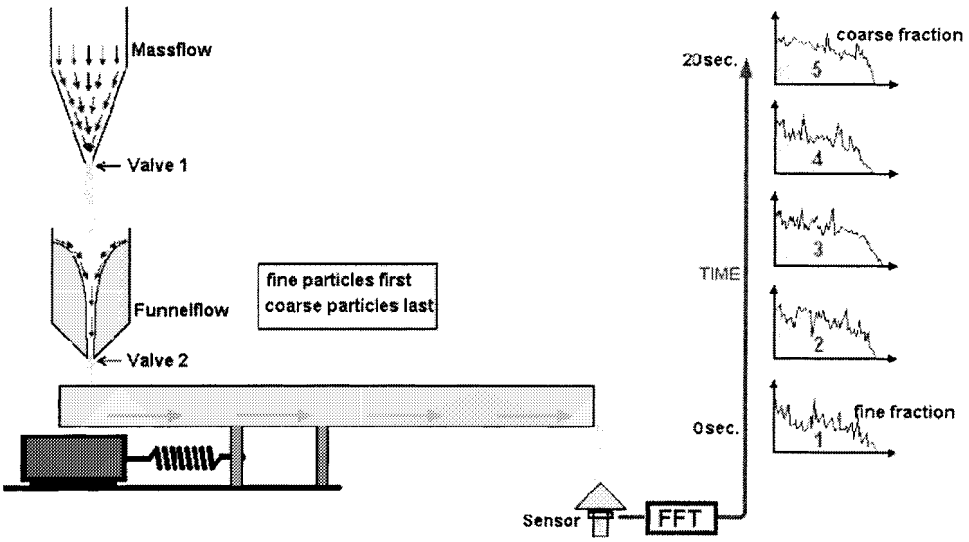

Figure 10. Schematic illustration of the new approach for prediction of particle size distribution in powder mixtures, called MS3WD (maximum segregation three-way decomposition). The upper silo is termed silo 1, the lower one silo 2.

NEW APPROACH

New approach—experiments

A new way of doing exactly the same experiments simply helps the powder to segregate as much as possible, while measuring the acoustic signals for an extended segregated series of part-samples (Figure 10).

The powder sample is first poured into silo 1, which is a so-called mass flow silo. When the particles are flowing out from silo 1 to silo 2, they will segregate, because the larger particles tend to roll out against the wall in silo 2 and the finer particles tend to accumulate in the middle section. This type of silo discharge flow segregation is a well-known feature within powder science and technology, in which Herculean efforts are spent in order to reduce this unwanted phenomenon [8]. The present new approach, MS3WD (maximum segregation three-way decomposition), simply turns this unavoidable fact on its head so as to be able work for the measuring situation instead of against it.

Figure 11 shows a cross-sectional view of silo 2 when being filled with a mixture of particles of different sizes.

Silo 2 is a so-called funnel flow silo [8] and will cause the fine particles (middle section) to come out first when valve 2 is opened. The last powder out of silo 2 is the coarse particles, closest to the walls. The discharged powder is continuously transported from silo 2 to the sensor by the vibrating slide, just as in the earlier experiments. The first acoustic recordings will overall represent the finer fractions, while the latter/last recordings (more) represent the coarse particles in the mixture. This set-up has been designed so as to allow the original batch sample to become as segregated as possible, also greatly helped by the vibrating slide, which furthermore has been extended relative to the earlier configurations so as to enhance the flow segregation even further.

Clearly, this grain size polarization will be attained only to some degree, and the overall separation of the initial sample into the desired finer/larger fractions will represent a continuous grading.

Copyright © 2000 John Wiley & Sons, Ltd.

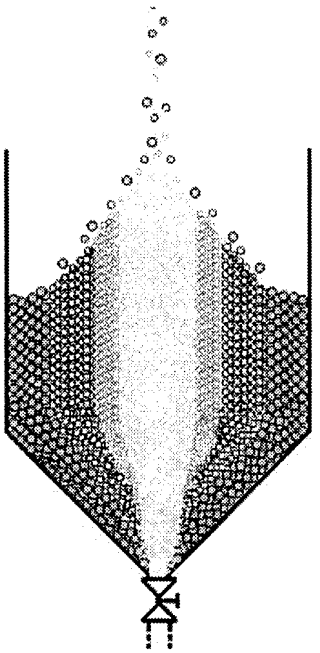

Figure 11. Cross-section of silo 2 when a mixture of different particle sizes is filled from the top of the silo. Coarser fractions accumulate along the walls, finer fractions towards the centre.

However, overall, a significantly enhanced segregation effect will be achieved, and this is all that is needed to crack open this very difficult problem anew.

The samples introduced into silo 1 must of course all have the same volume. In this experimental set-up we assume that the initial sample deposited in silo 1 is fully representative [9].

For batch processes this is a reasonable assumption, but for continuous flow processes the sampling of the flowing mixture stream may often be very difficult.

Figure 12 shows a typical profile of the segregated outcome of discharging silo 2.

The different 'time-spaced' acoustic effect spectra are illustrated schematically to the right in Figure 10. When the whole powder sample has reached the sensor, it has now been recorded by a sufficiently large number of spectra (instead of the five shown here in the illustration, we used 15 or 56 in the experiments reported below). Together, these spectra represent the whole powder mixture as a compound 'fingerprint' series. The segregation problem has been eliminated as far as possible; for every 0·04 s recording, a significantly more homogeneous sample is now reaching the sensor head per unit time interval. Because of this maximized segregation homogenization of the instantaneous part-samples, also the particle size ratio between coarse and fine particles, *D/d*, can now be much larger, so this is also no longer a limiting problem. We have estimated that *D/d* can now reach levels of 3–5 before severe limitations set in, whereas earlier the *D/d* window was restricted to 1–2·5. Follow-up experiments are currently under way in order to map these improved relationships in greater detail.

MS3WD experiments—two components

The experimental design for a lead-in experiment with two-component mixtures is shown in Figure 13. The powders used in this experiment are mixtures of quartz sand particles with the same density of

Copyright © 2000 John Wiley & Sons, Ltd.

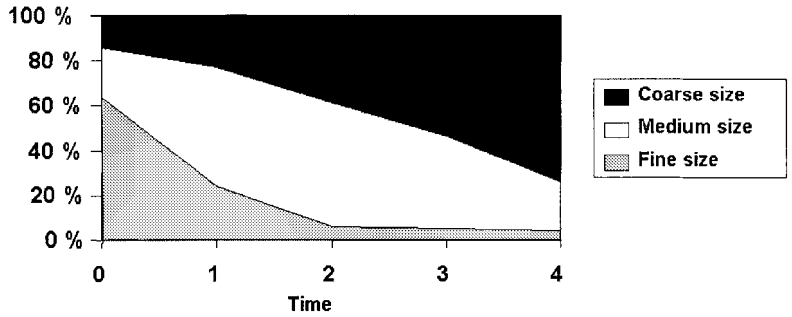

Figure 12. Segregated outcome of silo 2 when a three-component mixture is filled from silo 1; see also Figures 10 and 11. The valve at the bottom of the silo opens at time 0. Representative experimental data.

size fractions A and B (see Figure 6). Note the large fraction separation A/B. These simple two-component series are used in our ongoing work dealing with optimization of a new series of acoustic sensor configurations only.

Acoustic sensors used in the two-component experiments

All earlier work on acoustic chemometric powder mixture characterization has used the original cone-shaped accelerometer heads depicted in Figures 2, 4, 5 and 10; the cone concept was the original contribution of our distinguished collaborator Mr Bjørn Hope [3]. We are currently developing a series of new acoustic sensor configurations. Two of the new acoustic sensors were used in the two-component experiments: a microphone-based and an alternative accelerometer-based sensor arrangement.

The accelerometer-based sensor is a miniature high-frequency accelerometer glued onto a stiff plastic membrane with ceramic cement. The membrane has an angle of 45 ° to prevent accumulation of powder on the surface of the membrane. The accelerometer-based sensor can be seen in Figure 14.

The microphone-based sensor is a high-frequency microphone mounted through a hole in a bottom plate. The top of the sensor is now a hemisphere of thin, stiff plastic. The powder particles impact on the surface of the hemisphere and induce sound waves inside the hemisphere, which are detected by

Exp.#	A (125-150µm)	B (250-300µm)
1	100%	0%
2	90%	10%
3	80%	20%
4	70%	30%
5	60%	40%
6	50%	50%
7	40%	60%
8	30%	70%
9	20%	80%
10	10%	90%
11	0%	100%

Figure 13. Experimental design for two-component MS3WD mixtures (100% = 70 g).

Copyright © 2000 John Wiley & Sons, Ltd.

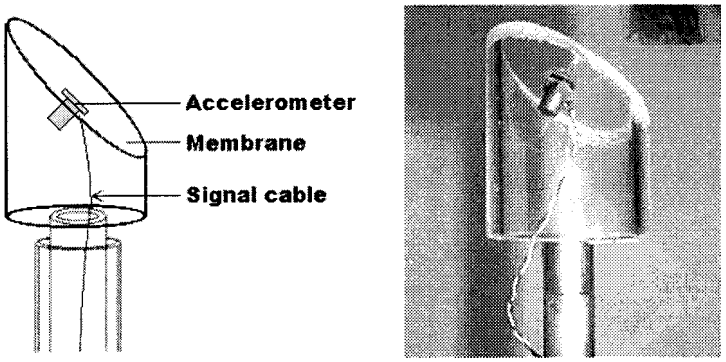

Figure 14. The accelerometer-based sensor used in the two-component experiments.

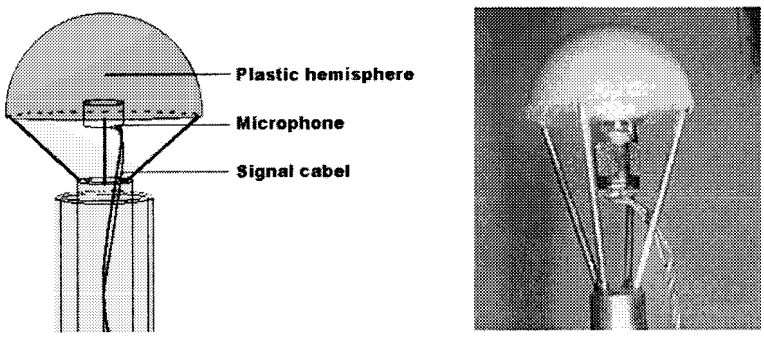

Figure 15. The microphone-based sensor used in the two-component experiments.

the microphone. This hemispherical volume is hermetically sealed. The microphone-based sensor can be seen in Figure 15.

RESULTS

Two-component MS3WD mixtures—results

The results from standard PLS-R multivariate calibrations using these two new sensors were almost identical, with the accelerometer-based sensor performing slightly better, so these are the only results presented here. There are parallel studies of five to seven other novel sensor configurations which will be presented elsewhere.

The characterization of each sample resulted in 15 'time-span' acoustic effect spectra, each an average of 150 of the individual 0·04 s unit measurements. Each final acoustic spectrum contains 1024 frequencies. The total number of variables for each powder sample was thus $15 \times 1024 = 15\,360$ in the unfolded [10–14] two-way PLS mode.

Results from the two-component experiment showing the improvement obtained can be seen in Figure 16, to be compared with Figures 7–9. The new models are of course validated with full cross-validation, as there are only 11 samples for these studies (each an average of five replicates). Two PLS components were found optimal for both fractions A and B, which is no surprise in the context of one mixing series and (at least) one compensating component.

Copyright © 2000 John Wiley & Sons, Ltd.

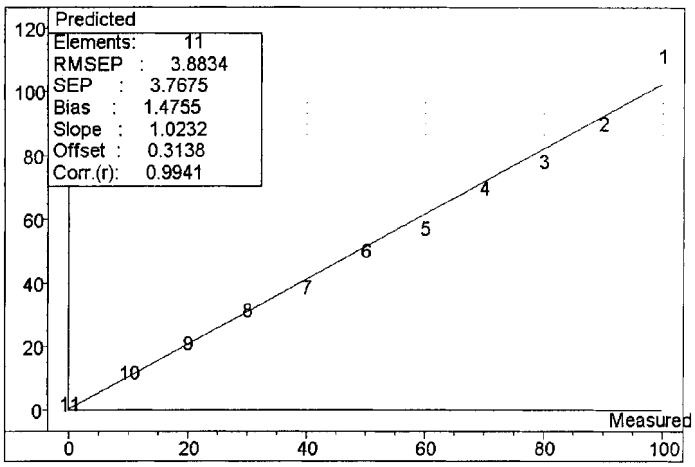

Figure 16. Unfolded two-way PLS-predicted versus measured plot/statistics for fraction A (125–150 μm) in MS3WD two-component mixtures.

These results by themselves represent a major improvement. The precision involved is increased relative to all earlier results, now being 3·9% for both fractions. This factor-of-two improvement comes about exclusively because of the new MS3WD approach, as all other experimental conditions and parameters were identical. The overall accuracy and precision in Figures 16 and 17 is very satisfactory, with biases of 1·50 and −1·50, offsets of 0·30 and −2·60 respectively and $r^2 = 0{\cdot}988$, relative to a measurement range of 0–100% (abs.).

These comparative experiments with the new approach so far include only two-component mixtures, and therefore the experiment is (much) simpler than the many three-component experiments done earlier. We also have to do experiments with three components in order to compare results on the same basis as earlier. Turning to the more realistic three-component mixtures, unfolding two-way PLS-R could of course still be used, but the essence of the new MS3WD approach is related to using a true three-way PLS solution [10–14], which will be presented below.

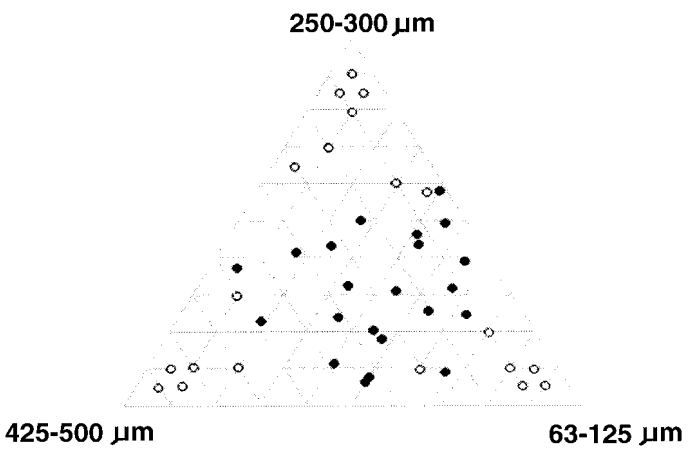

Figure 17. Full experimental design for the three-component MS3WD experiments; see text for further details.

Copyright © 2000 John Wiley & Sons, Ltd.

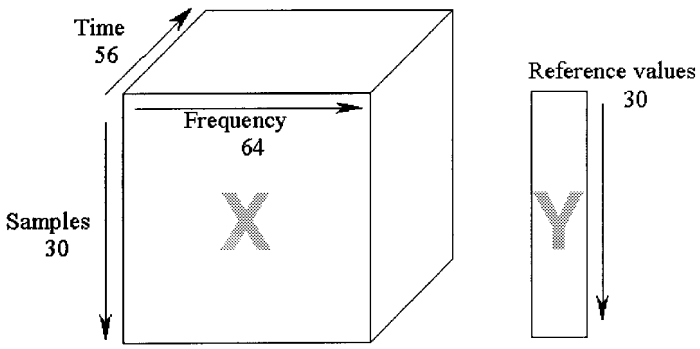

Figure 18. Data array configuration of the three-way PLS calibration experiments.

Three-component MS3WD mixtures—results

From preliminary experimental runs we concluded that we needed improved time resolution; therefore the recording parameters used earlier in the two-component set-up were changed as follows.

The acoustic recordings of each sample were this time done by measuring 56 'time-span' acoustic effect spectra, but now each is an average of 40 unit recordings only, and each acoustic spectrum now contains only 64 frequencies. The total number of variables for each powder sample would be $56 \times 64 = 3584$ if an unfolding option were to have been used here also.

The experimental design for the three-component mixture experiments is shown in Figure 17. The powders used in this experiment are again mixtures of quartz sand particles with the same density. The total number of experiments is 42 [15].

The layout of this design is composed of a central 'core', which is a renormalized 'random design' [3] (full circles), to which we have added a manual 'end-member design' (open circles), also renormalized to 100% for each sample. The all-important aspect of whichever design is adopted here is that the compositional space be well spanned. The compositional coverage of all pertinent experimental calibration and validation data sets can be fully appreciated in Figures 21, 23 and 25 below.

100% corresponds to 70 g of powder mixture, which was found to be adequate for the MS3WD characterizations. The duration of a full time-span recording series was approximately 40 s for all samples.

The three-way PLS-R [10–14] results for the three-fraction experiments can be seen in Figures 18–25. For this experiment we used 30 samples, randomly selected, as the calibration data set and the remaining 12 samples as a test set. We of course used different test sets for each of the three *Y*-variables, corresponding to the three size fractions A, B and C. From these test set validations, four and five components were found optimal for the three size fractions.

The three-way PLS-R data array configuration for multivariate calibration of the acoustic chemometric three-component mixture size prediction experiments is seen in Figure 18.

MS3WD results for fraction A (63–125 μm)

The results for the test set-validated three-way solution for fraction A (63–125 μm) can be seen in Figures 19–21.

Validation results are obtained using four components; >90% *Y*-variance explained by 85% *X*-variance. The loading weight relationships will be discussed further below. In the predicted versus measured plot, one test set outlier was detected. Outliers may be found either in the calibration or in

Copyright © 2000 John Wiley & Sons, Ltd.

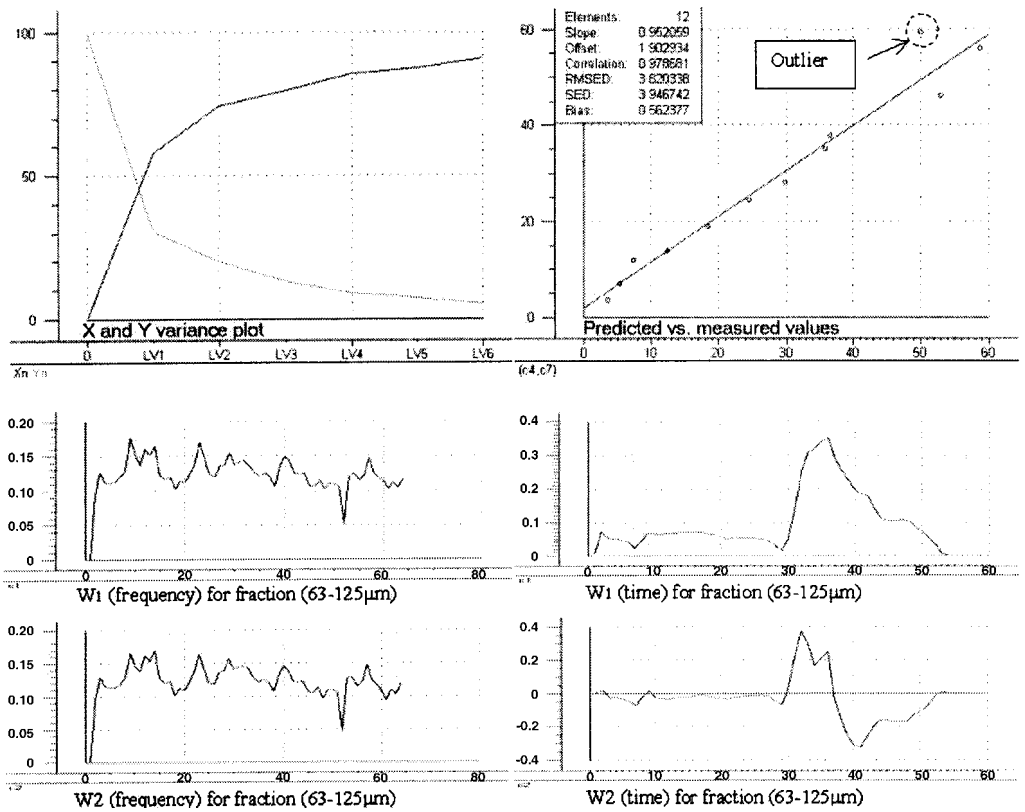

Figure 19. Results for the test set-validated three-way PLS solution for fraction A (63–125 μm) with four components. W_1 denotes the loading weights for component 1. *W* (time) denotes the loading weights for the time direction and *W* (frequency) for the frequency direction of the three-way data. RMSED means the same as RMSEP.

the true test data set. This sample has an extremely low fraction of coarse particles; in fact, there are no other samples in the entire calibration data with this small amount. Removing this sample from the validation data, the corrected validations in Figure 20 thus pertain to 11 samples in the test set. We choose to present both results here. There are no similar outliers in the results for the other two size fractions. The 12-sample test validation results in a precision of 5·45% (3·82 g), while the corrected validation estimates the relative% RMSEP as 3·92% (2·75 g), which is close to the level for the unfolded two-way PLS prediction (Figure 16). Thus we are close to the same level of precision with the realistic three-component predictions as for the earlier simplistic two-component results for fraction A.

The coverage of the calibration and test set samples for fraction A is shown in Figure 21.

MS3WD results for fraction B (250–300 μm)

The results for a similar test set-validated three-way solution for fraction B (250–300 μm) can be seen in Figures 22–23.

For this situation, one would expect the largest uncertainties to arise when predicting size fractions for fraction B; this is very well established from our extensive earlier three-component studies [6].

Copyright © 2000 John Wiley & Sons, Ltd.

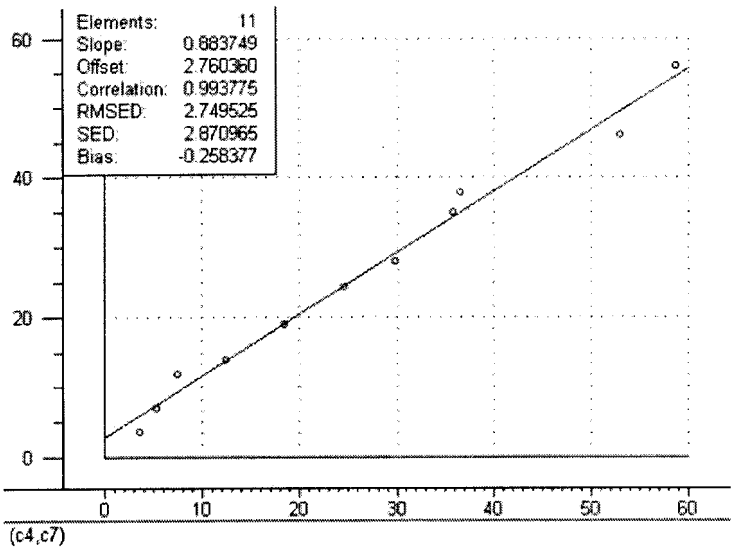

Figure 20. Predicted versus measured for fraction A (63–125 μm). One outlier removed, $r^2 = 0{\cdot}98$. RMSED means the same as RMSEP.

Test set validation estimates that five PLS components are needed in this more complex intermediate context. With five components (see Figure 22) the precision is 8·14% (5·7 g), clearly high.

Calibration and test set samples for fraction B (250–300 μm) are shown in Figure 23.

MS3WD results for fraction C (425–500 μm)

The results for the test set-validated three-way prediction for fraction C (425–500 μm) can be seen in Figure 24.

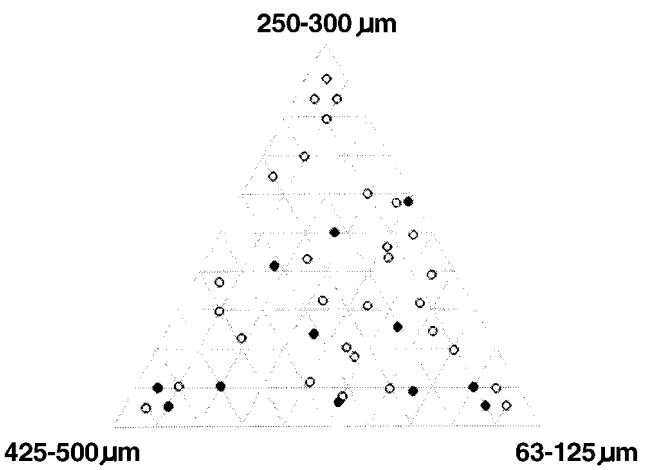

Figure 21. Test set (full circles) for fraction A (63–125 μm).

Copyright © 2000 John Wiley & Sons, Ltd.

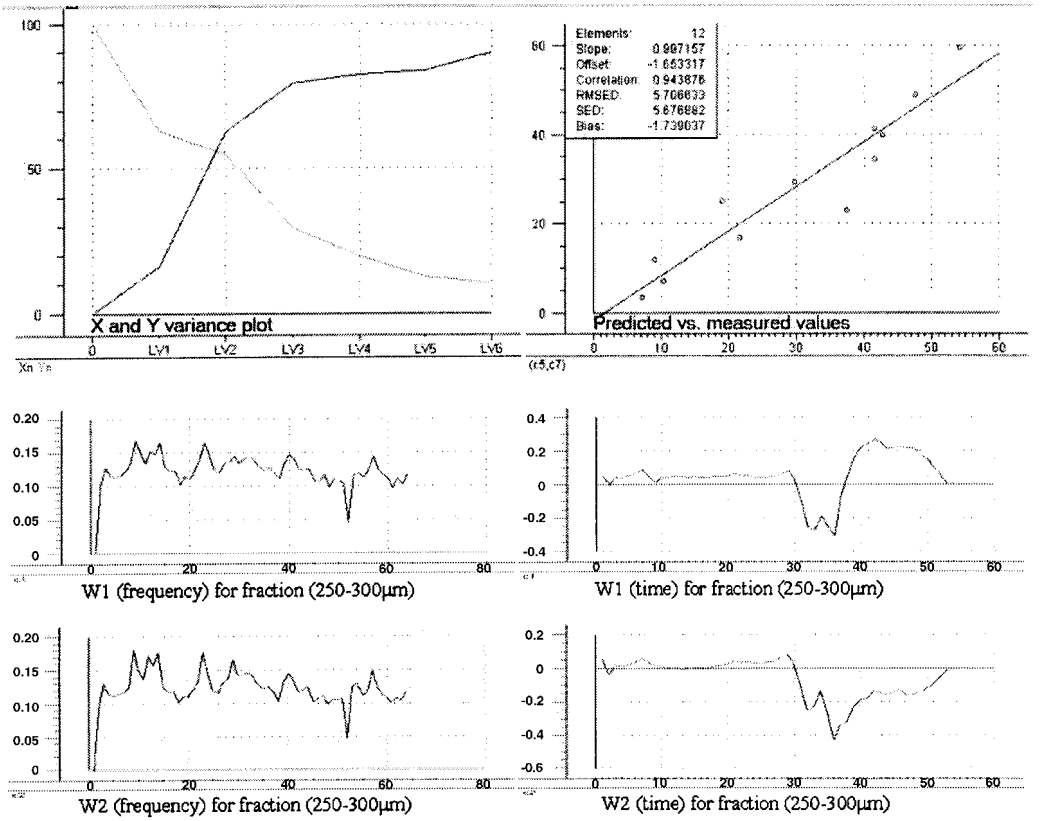

Figure 22. Results for the test set-validated three-way PLS solution for the intermediate size fraction B (250–300 μm) with five components. $r^2 = 0{\cdot}89$. W_1 denotes the loading weights for component 1. *W* (time) denotes the loading weights for the time direction and *W* (frequency) for the frequency direction of the three-way data. RMSED is the same as RMSEP.

For this coarsest size fraction predicted by the new MS3WD approach, the test set-estimated precision comes to 4·8% (3·3 g) (Figure 24).

Calibration and test set samples for fraction C (425–500 μm) are shown in Figure 25.

These results correspond to our earlier three-component experiments w.r.t. the relative accuracy and precision obtained for the A/B/C relationships, only now with greatly improved numerical prediction statistics.

DISCUSSION

We have employed three different, randomly chosen test set validations for the three size fractions, for which individual MS3WD PLS calibrations have been carried out; there were 30 calibration data set samples and 12 (11) test set samples in each case, corresponding to a training/test sample ratio of 2·5. We did not press the test set estimates of the optimal number of PLS components to the absolute maximum; from Figures 19, 22 and 24 it may be appreciated that four, five and four components correspond to only reasonable '*Y*-variance minima', taking the 2·5 sample ratio into account.

On the other hand, one might argue that a very first implementation of a completely new technique

Copyright © 2000 John Wiley & Sons, Ltd.

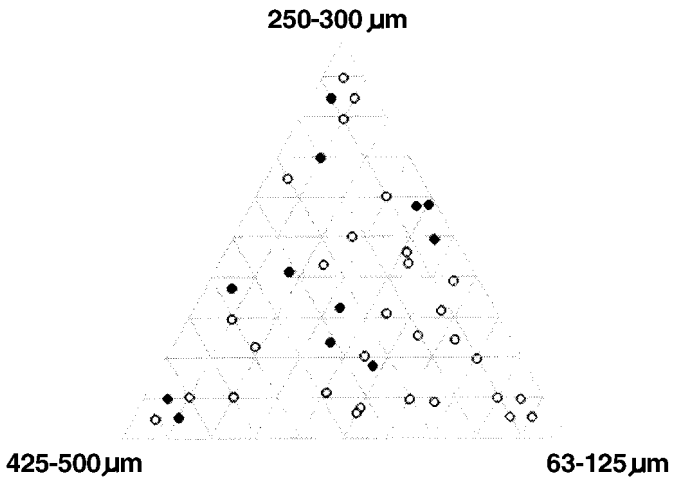

Figure 23. Test set (full circles) for fraction B (250–300 µm).

may not necessarily be expected to reach the ultimate precision and accuracy specifications set in the introduction in just one go. For one thing, the signal-recording parameters (number of replicate averages to make one record; number of 'time-span' spectra; spectral resolution; etc.) have not yet been systematically optimized, as this undertaking is critically dependent upon which sensor type is employed; here we have only been able to present results for two sensors. There are still some five to seven other sensor types which are scheduled to undergo identical treatment as the ones reported here, before we can make any final comparative judgements. Systematic studies are currently under way and will be presented elsewhere in due course.

We do, however, have more than enough results in this first foray to meaningfully compare this new approach with the best of the existing methodology.

The absolutely very best three-component precision obtained earlier, without the MS3WD approach, was in the 6%–10% range; compare Figures 7–9 [6]. It must be remembered though that these were all internal cross-validation results and therefore necessarily on the optimistic estimation side. There were also many other results reported earlier [6], some for example pertaining to both four- and five-component systems (again without the MS3WD approach). An overall average precision level for all these results comes to some 6%–10% precision, but with rather large positive variations on top. This is where the earlier development of the acoustic chemometric powder mixture size distribution prediction work came to a halt—slowed down by both the self-damping and *D/d* window bracket obstacles as well as by the crippling flow segregation during delivery of the sample to the sensor head.

For the present MS3WD results the more realistic test set precision estimates are 3·9% (2·75 g), 8·1% (5·7 g) and 4·7% (3·3 g) for fractions A, B and C respectively. There has been no significant method optimization possible yet, pending the future extensive systematic sensor/signal-recording work, but by referring to the experiences learned from all our other acoustic chemometrics work, it would not appear unreasonable to expect the precision levels to be reducible by some 30%–40% [1–3]. This would bring them right down to the industrial specification range of around 2%–5%. We are thus (more than) happy with the above first results; indeed, Figures 20, 22 and 24 are very acceptable compressed format validation results. Some salient statistics, satisfactory for any multivariate calibration validations can be quoted: the correlation coefficients (r^2) for the fitted prediction/

Copyright © 2000 John Wiley & Sons, Ltd.

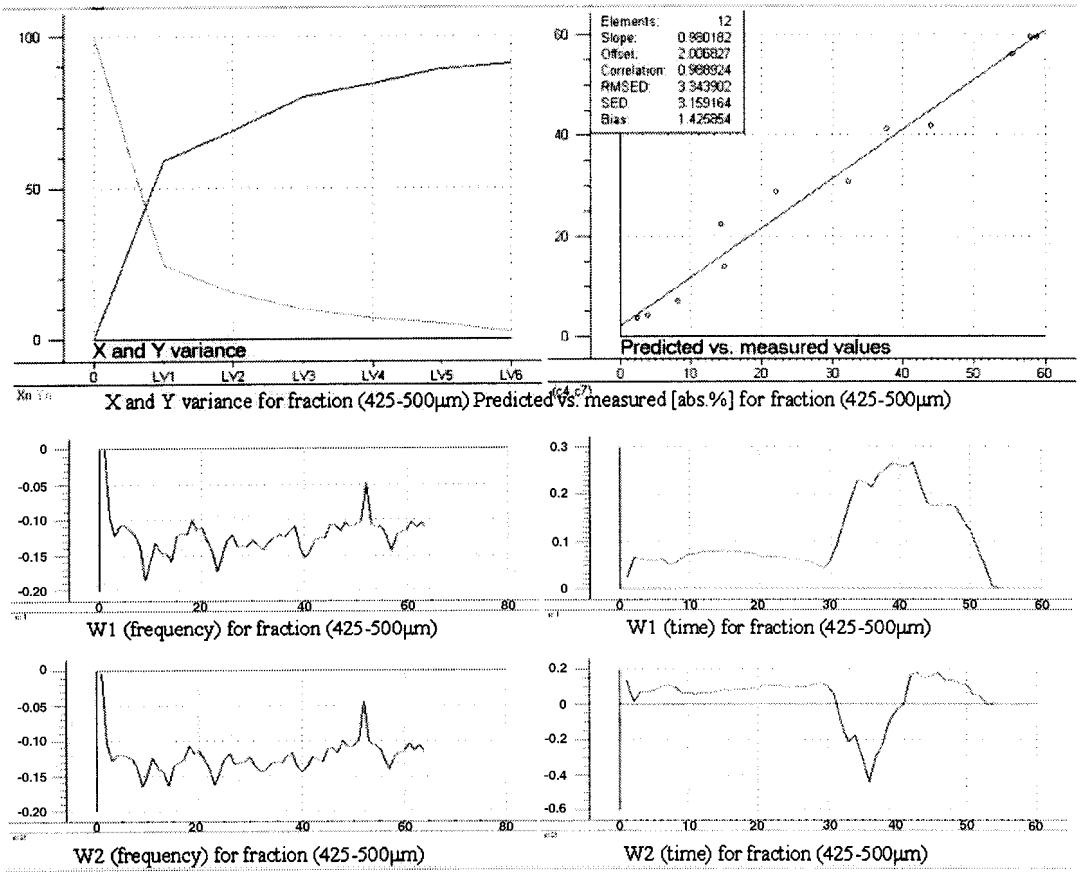

Figure 24. Results for the test set-validated three-way PLS solution for fraction C (425–500 μm) with four components. $r^2 = 0{\cdot}96$. W_1 denotes the loading weights for component 1. *W* (time) denotes the loading weights for the time direction and *W* (frequency) for the frequency direction of the three-way data. RMSED is the same as RMSEP.

measured regressions are 0·986, 0·900 and 0·978 respectively, while the regression line slopes reach 0·88, 0·95 and 0·98, all with only insignificant offsets.

Why is this new MS3WD approach working so much better on the realistic multicomponent cases, reducing the self-damping and the *D/d* ratio problem?

Some insight into this may be gleaned from inspection of the three-PLS-component loading weights for the prediction models pertaining to fractions A, B and C. From Figures 19, 22 and 24 it will be appreciated that the first PLS component plays the most dominant role (less so for the complex intermediate-size-fraction case). For three-way PLS solutions there is a set of loading weights for both the spectral and time domains, but the important information in this context resides in the time direction, corresponding to the extended vibrating delivery slide.

The loading weight plots for the time direction for all three fractions are displayed simultaneously in Figure 26. This plot shows that it is the time interval from 30 to 50 (time 60 corresponds to the 40 s reported above) which is most important for modelling all three fractions. Not surprisingly, for both the finest and coarsest size fractions the W_1 spectra are rather similar on a first comparison, harking

Copyright © 2000 John Wiley & Sons, Ltd.

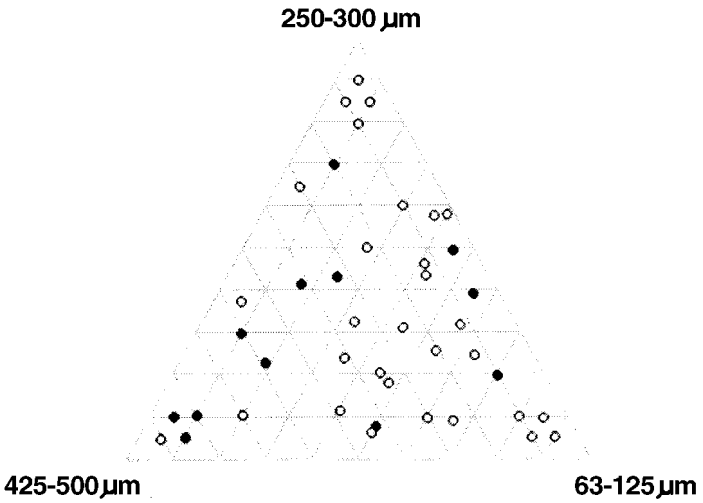

Figure 25. Test set samples for fraction C (425–500 µm).

back to a two-end-member situation in which less of one fraction perforce means a one-to-one increase in the other. On closer inspection, there are of course also important second-order differences between fractions A and C (see Figures 19 and 24), which will be interpreted in more detail first in the ongoing comparative sensor configuration studies. Fraction B loading weights are very distinct.

The powder samples which have a large amount of fine particles use less time through the entire MS3WD set-up than samples with smaller amount of fines. This is so because small particles flow more easily through the bottom hole of silo 2, while also travelling faster along the vibrating slide. The samples with a high concentration of coarse particles are the slowest to go through the silo. It is therefore these samples which typically have up to 50 acoustic effect spectra each. By way of contrast, the samples with minor amounts of coarse particles produce only about 30 'time-span' acoustic effect spectra. It follows that even the number of non-zero spectra in itself is important for the MS3WD characterization of all three fractions. Thus both the number of and the individual acoustic effect spectra are important for the quantitative description of the particle size distribution. Clearly, without the three-way data facility the new approach would not even get off the ground.

The loading weight plots for the frequency direction are very similar (see Figures 19, 22 and 24), indicating that the most important frequencies in all these spectra are rather invariant over all three size fractions modelled. It is thus the new time domain resolution which is responsible for the breakthrough reported here. Much work remains.

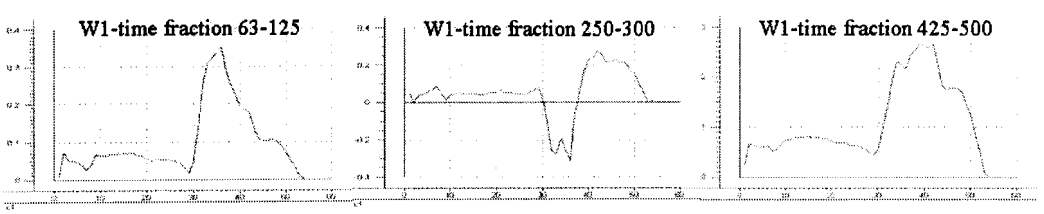

Figure 26. Comparative loading weights W_I in the time direction for all three fractions A, B and C.

Copyright © 2000 John Wiley & Sons, Ltd.

CONCLUSIONS

Two-way PLS results

The new MS3WD two-component, unfolded (two-way) 'predicted versus measured' validations for the three present size fractions show that the new approach is more precise than the relatively simple basic approach used in all earlier experiments (Figures 7–9 and 16). Precision is improved for these simple systems (by an order of magnitude).

Three-way PLS results

We cannot compare the results from the earlier experiments directly on the same basis as the results from the new method, because the latter is test set validated while the earlier experiments were cross-validated. Test set validation is **always** to be preferred! The new test set validation results, pertaining to these first implementations only, already have the precision down to half the earlier estimated levels.

The results obtained in this first study indicate that the maximum segregation three-way decomposition (MS3WD) approach is a promising new way to handle samples where the size ratio between the coarse and fine particles, *D/d*, was earlier prohibitively large.

The most important feature in this study is that the phenomenon which was earlier *the problem* is now seen to be *the solution*. Both the flow segregation and the contrast ratio problem have been solved by the MS3WD approach; there still remain several obvious and interesting engineering optimizations, only some of which were outlined above.

ACKNOWLEDGEMENTS

We are grateful to Mr Bjørn Hope of Sensorteknikk A/S, Oslo for his inspiration and contributions to acoustic chemometrics. The concepts of the silo and vibrating slide delivery systems, as well as the cone-shaped sensor configuration, are his original concepts.

REFERENCES

1. Halstensen M, de Silva SR, Esbensen KH. Acoustic monitoring of pneumatic transport lines—from noise to information. *KONA #16*, 1998;170–178.
2. Esbensen KH, Halstensen M, Lied TT, Saudland A, Svalestuen J, de Silva SR, Hope B. Acoustic chemometrics—from noise to information. *Chemometrics Intell. Lab. Syst.* 1998; **44**:61–76.
3. Esbensen KH, Hope B, Lied TT, Halstensen M, Gravermoen T, Sundberg K. Acoustic chemometrics for fluid flow quantifications—II: A small constriction will go a long way. *J. Chemometrics* 1999; **13**:209–236.
4. Ifeachor IC, Jervis BW. *Digital Signal Processing, a Practical Approach*. Addison-Wesley: Reading, MA, 1993.
5. Martens H, Næ s T. *Multivariate Calibration*. Wiley: Chichester, 1989.
6. Berdal A. Eksperimentell kjemometrisk karakterisering av kornstørrelsesfordeling av sandblandinger-videregående studier mht. utvikling av en hw/sw prototype for in-line industriell måleteknologi. *MSc Thesis*, 1997 (in Norwegian).
7. Box GEP, Hunter WG, Hunter JS. *Statistics for Experimenters*. Wiley: New York, 1978.
8. Mosby J, de Silva SR, Enstad GG. Segregation of particulate materials: mechanisms and testers. *KONA #14*, 1996;31–43.
9. Gy P. *Sampling for Analytical Purposes*. Wiley: Chichester, 1998.
10. Bro R. Multi-way analysis in the food industry. *Doctoral Thesis*, 1998.
11. Bro R. Multi-way calibration, multi-linear PLS. *J. Chemometrics* 1996; **10**: 47.
12. Geladi P. Analysis of multi-way (multi-mode) data. *Chemometrics Intell. Lab. Syst.* 1989; **7**:11.
13. Smilde AK. Comments on multilinear PLS. *J. Chemometrics* 1997; **11**:367.
14. Smilde AK. Multi-way regression models. *Internal Report*, University of Amsterdam, 1997.
15. Adams D. *The Hitch-hiker's Guide to the Galaxy*. Pan Books: London, 1979; chap. 27.

Copyright © 2000 John Wiley & Sons, Ltd.